General Disclaimer

One or more of the Following Statements may affect this Document

- This document has been reproduced from the best copy furnished by the organizational source. It is being released in the interest of making available as much information as possible.

- This document may contain data, which exceeds the sheet parameters. It was furnished in this condition by the organizational source and is the best copy available.

- This document may contain tone-on-tone or color graphs, charts and/or pictures, which have been reproduced in black and white.

- This document is paginated as submitted by the original source.

- Portions of this document are not fully legible due to the historical nature of some of the material. However, it is the best reproduction available from the original submission.

NASA TECHNICAL MEMORANDUM

NASA TM X-73466

NASA TM X-73466

TORNADOES AND OTHER ATMOSPHERIC VORTICES

by Robert G. Deissler
Lewis Research Center
Cleveland, Ohio 44135

TORNADOES AND OTHER ATMOSPHERIC VORTICES

by Robert G. Deissler
Lewis Research Center

Abstract

The growth of random vortices in an atmosphere with buoyant instability and vertical wind shear is studied analytically. A study is also made of the velocities in a single gravity-driven vortex; a frictionless adiabatic model which is supported by laboratory experiments is first considered. The effects of axial drag, heat transfer, and precipitation-induced downdrafts are then calculated. Heat transfer and axial drag tend to have stabilizing effects; they reduce the downdrafts or updrafts due to buoyancy. It is found that downdrafts of tornadic magnitude might occur in negatively-buoyant columns. The radial-inflow velocity required to maintain a given maximum tangential velocity in a tornado is determined by using a turbulent vortex model. Conditions under which radial-inflow velocities become sufficiently large to produce tangential velocities of tornadic magnitude are determined. The radial velocities in the outer regions, as well as the tangential velocities in the inner regions may be large enough to cause damage. The surface boundary layer, which is a region where large radial inflows can occur, is studied, and the thickness of the radial-inflow friction layer is estimated. Finally, a tornado model which involves a rotating parent cloud, as well as buoyancy and precipitation effects, is discussed.

1. Introduction

Observations of tornadoes have been made for many years, the first known photograph having been taken in 1884 (Science, 1972; Fig. 1). The destructive aspects of tornadoes are well known. Still, there appears to be little agreement about their dynamics. The lack of agreement is, of course, at least partly due to the devastating nature of tornadoes and the consequent difficulty of making

meaningful measurements. Less devastating atmospheric vortices such as dust devils and waterspouts might be profitably studied, but there is no assurance that their mechanisms are the same as those of tornadoes. Thus theories and laboratory experiments should play an important role in tornado research.

Capabilities for observing the stronger vortices have, of course, been steadily increasing (Preprints of Papers, Ninth Conference on Severe Local Storms, 1975). This is fortunate, since theories and laboratory experiments by themselves are insufficient. Thus we may perform an analysis of vortex behavior, devise an experiment to test the analysis, and get agreement between the two. However, there is no assurance that the results will apply to real atmospheric vortices, unless we know that the assumptions made in the theory and experiment apply to vortices in the atmosphere. In order to make progress, theory, laboratory experiments, and field observations are all indispensible.

Several aspects of atmospheric vortices are considered herein, including their production, structure, and maintenance. Although the emphasis will be on tornadoes, much of the discussion will also be applicable to smaller atmospheric vortices, such as dust devils and waterspouts.

Throughout the paper we will use the Boussinesq approximation in the equations of motion of the fluid; that is, the fluid will be considered as incompressible, except where density differences affect the buoyancy, and the density differences will be taken to depend only on the temperature. However, the effects of moisture and vertical pressure differences on the buoyancy can usually be accounted for by using suitable potential temperatures in place of ordinary temperatures in the equations (e.g., Kuo, 1966). The potential temperature is defined as the temperature attained by the fluid when it is compressed adiabatically to a standard pressure. The fluid may contain condensing or evaporating liquid. If the potential temperature is independent of altitude, there will be no buoyancy force acting on a displaced fluid element. Thus for the results to be applicable to atmospheric

vortices, the temperatures in the analysis should be considered to be potential temperatures.

In the tornado models considered, axial symmetry will be assumed. Although there may be significant nonsymmetric aspects of tornadoes, most of the important features should show up in an axisymmetric model.

2. Growth Of Random Vortices In An Unstable Atmosphere With Vertical Shear

Extensive studies of tornado and funnel-cloud occurrences (Wills, 1969; and Modahl and Gray, 1971) have shown a high degree of correlation of those occurrences with atmospheric instability and vertical wind shear. Wills has stated that it does not appear coincidental that the major tornado-producing region of the world (the eastern two-thirds of the United States) is the only area where strong vertical wind shears and strong potential instability are frequently simultaneously present. Thus one approach to the study of tornado occurrences might be to analyze the growth of random vortices under these conditions.

Such an analysis has already been carried out in a study of the growth due to buoyancy of a homogeneous turbulence (or vortex distribution) with shear (Deissler, 1967, 1971). The self-interaction between the turbulent eddies (random vortices) was assumed to be small compared with their interaction with the mean temperature and velocity gradients. (This assumption does not necessarily imply that the random vortices are weak.) That case is of interest here, since we are more concerned with the interaction of the vortices with the mean gradients than we are in their interaction with one another. The initial distribution of vortices is assumed isotropic, but their distribution becomes anisotropic under the influence of the mean gradients. Although this approach considers the occurrence of atmospheric vortices as random events, it should show conditions under which such occurrences are highly probable. From a forecasting standpoint this may be all that can be hoped for; the prediction with certainty of the exact time and place of a tornado occurrence may not be feasible.

Results for the growth of the vorticity and size of typical vortices are shown in Fig. 2 for a Richardson number Ri based on vertical temperature and velocity gradients of -10. That is a typical Richardson number for tornado occurrence (Wills, 1969), where $(Ri \equiv \beta g(dT/dz)/(dU/dz)^2)$. (The vorticity of a typical vortex is taken here as the root mean square vorticity at the wave number where the vorticity spectrum is a maximum. The size of a typical vortex is taken as the reciprocal of the wave number at which the vorticity spectrum is a maximum.) The quantity β is the thermal expansion coefficient, g is the gravitational body force per unit mass, dT/dz is the vertical gradient of potential temperature (negative for unstable conditions), dU/dz is the vertical gradient of horizontal velocity (vertical wind shear), and κ_0 is a characteristic wave number (reciprocal of size) for the initial vortices. The value of κ_0^* shown in the figure is somewhat arbitrary but should be of the right order of magnitude for an unstable atmosphere if the vortices under consideration are themselves turbulent. In that case the kinematic viscosity ν will be replaced by a much larger turbulent viscosity (Deissler and Perlmutter, 1960).

The results in Fig. 2 show that both the vorticity and size (particularly the vorticity) of a typical random vortex increase considerably with dimensionless time (dU/dy ≈ 0.003 sec^{-1}). This result is illustrated schematically by the vortices sketched in Fig. 3 for an early and a later time. Thus, in agreement with the observational studies of Wills and of Modahl and Gray, the theoretical results show that the simultaneous presence of strong potential instability and vertical wind shear are favorable for the development of atmospheric vortices. The results also show the importance of the time element in the strengthening of atmospheric vortices. In addition to the Richardson number, a dimensionless time (dU/dz)t is also an important parameter. (Alternatively we could, by multiplying (dU/dz)t by (Richardson number)$^{1/4}$, consider the dimensionless time to be $[\beta g(dT/dz)^{1/2}t]$.) Thus if the conditions of strong potential instability and

vertical wind shear persist for a long enough time, the occurrence of strong at-
mospheric vortices will become highly probable.

One point which might be emphasized is that in this model we have not had
to postulate a large supply of cyclonic or anticyclonic vorticity. The net vorticity
can in fact be zero, some of the vortices being cyclonic and some of them anti-
cyclonic. On a large scale, this generation of vortices may be similar to the
split of a thunderstorm into anticyclonic and cyclonic storms (Fujita and
Grandoso, 1968). Of course the large vortices (tornadoes or tornado cyclones)
are more likely to be cyclonic because of the effect of earth rotation. Thus
lines of tornadoes (cyclonically rotating clouds) tend to move away from squall
lines (nonrotating clouds)(Fugita, 1975). But the smaller dust devils are nearly
as often anticyclonic as cyclonic. (According to this point of view the movement
of cars on the left instead of the right side of the road, to generate less cyclonic
and more anticyclonic vorticity (Isaacs et al, 1975), would not appreciably in-
fluence the total number of tornadoes, but it may decrease the proportion of
cyclonic to anticyclonic ones. In order to do that it may be necessary for the
road to be hotter than the surroundings (Manton, 1976).)

Can we conclude, then, that vortices of tornadic intensity can be generated
and maintained by the mechanism considered in this section? They might be
generated in that way, but if they are like turbulent eddies, they will decay in
times on the order of a few multiples of r/v, where r is the vortex radius and
v is its velocity. Thus the Dallas tornado (Hoecker, 1960) had a radius at the
maximum tengential velocity of about 70 meters and a maximum tangential veloc-
ity of about 70 meters per second, so that its lifetime, if it is like a turbulent
eddy, would be on the order of a few seconds, a time much too short to be
realistic for tornadoes. On the other hand, a vortex having the same value of
radius times tangential velocity as the Dallas tornado (a measure of the vortex
strength), but a diameter of several miles, could have a lifetime on the order of

a few hours. Thus the large to. yclone or rotating parent cloud (Fugita, 1960) from which the tornado contracted, might have been similar to a turbulent eddy formed in the way considered in this section. But in order for a vortex of tornadic strength and size to be maintained, large radial inflows will be required (see section 5).

Another point which should perhaps be discussed is that buoyancy-irᵈ ced instability tends to produce horizontal vorticity (Deissler, 1967), whereas the vorticity in tornadoes tends to be more nearly vertical. However since only a small percentage of the vortices develop into tornadoes, it will be sufficient if at least some of them are not horizontal. Perhaps the reason vertical shear, as well as buoyancy, is apparently required for tornado development (Wills, 1969) is that vertical shear tends to produce more nonhorizontal vorticity than does buoyancy (Deissler, 1967).

Once a vortex has been generated in an apparently random fashion, as discussed in this section, we can consider its structure. We will now look at a vortex in more detail.

3. A Frictionless, Adiabatic Model

For the sake of simplicity we will consider first a frictionless vortex without heat transfer. The analysis given here is a generalization of that given by Deissler and Boldman (1974). The steady-state equations for the conservation of mass and momentum for an axially symmetric flow can be written, with the Boussinesq approximation, as (Landau and Lifshitz, 1959)

$$\frac{1}{r}\frac{\partial}{\partial r}(ru) + \frac{\partial w}{\partial z} = 0 \tag{1}$$

$$w\frac{\partial w}{\partial z} + u\frac{\partial w}{\partial r} = -\frac{1}{\rho}\frac{\partial(p - p_e)}{\partial z} - \beta g\left(T_{e0} - T + \frac{\partial T_e}{\partial z}z\right) \tag{2}$$

$$u\frac{\partial v}{\partial r} + w\frac{\partial v}{\partial z} + \frac{uv}{r} = 0 \tag{3}$$

and

$$u \frac{\partial u}{\partial r} + w \frac{\partial u}{\partial z} - \frac{v^2}{r} = -\frac{1}{\rho} \frac{\partial (p - p_e)}{\partial r} \tag{4}$$

where r and z are, respectively, the radial and vertical coordinates, u, v, and w are the radial, tangential, and vertical velocities, ρ is the density, p is the pressure, T is the potential temperature in the vortex, p_e is the equilibrium pressure, T_{e0} is the equilibrium temperature at z = 0, g is the acceleration of gravity, and $\beta = T^{-1}$ is the thermal expansion coefficient for the atmosphere. The last term in Eq. (2) is the buoyancy term, where the vertical temperature gradient in the surrounding atmosphere $\partial T_e/\partial z$, and T, are assumed constant. Let w = w(z) and v = v(r) within the vortex or region of interest. If the first two terms in Eq. (4) are small compared with the third term, as they probably are for most of a tornado (Hoecker, 1961), Eq. (4) shows that $p - p_e = (p - p_e)(r)$. (In the outer region, although the first term may not be small compared with the third, $p - p_e$ as calculated from Eq. (4) either with or without the first term, is small.) Equations (2) and (3) become

$$w \frac{\partial w(z)}{\partial z} = -\beta g \left(T_{e0} - T + \frac{\partial T_e}{\partial z} z \right) \tag{5}$$

and

$$\frac{\partial v(r)}{\partial r} + \frac{v(r)}{r} = 0 \tag{6}$$

Solution of Eq. (5), with the initial condition $w = w_0$ when z = 0 then gives, for the vertical velocity,

$$w = \pm \left[w_0^2 - 2\beta g(T_{e0} - T)z - \beta g \frac{\partial T_e}{\partial z} z^2 \right]^{1/2} \tag{7}$$

From Eqs. (1) and (7) we get, by using the condition that u is finite at r = 0,

$$u = \mp \frac{-\beta g\left[T_{e0} - T + (\partial T_e/\partial z)z\right]r}{2\left[w_0^2 - 2\beta g(T_{e0} - T)z - \beta g(\partial T_e/\partial z)z^2\right]^{1/2}} \tag{8}$$

Equations (7) and (8) show that for large z,

$$w = \pm(-\beta g\,\partial T_e/\partial z)^{1/2}\,z; \ u = \mp\frac{1}{2}(-\beta g\,\partial T_e/\partial z)^{1/2}\,r \tag{9}$$

whereas for small z,

$$w = w_0; \ u = \pm\beta g(T_{e0} - T)\,r/(2w_0) \tag{10}$$

Thus the radial velocity u can be large if w_0 is small and $T_{e0} - T$ is non-zero at $z = 0$. As will be seen in section 5, a large radial inflow is favorable for the maintenance of large tangential velocities.

From Eq. (6), we get

$$v/v_i = (r/r_i)^{-1} \tag{11}$$

where v_i is the tangential velocity at $r = r_i$. This equation applies reasonably well except for very small r, where friction becomes important (Deissler and Perlmutter, 1960). The important question of when tangential friction cannot be neglected will be considered in detail in section 5.

Although the vertical temperature gradient $\partial T_e/\partial z$ is important in the atmosphere, it's effect is hard to investigate in the laboratory. Thus, in order to see if the model considered here can give reasonable correspondence with laboratory results, we devised experiments where the buoyancy force was proportional to $T_{e0} - T$ (or to $\rho_{e0} - \rho$). For that case, along a streamline (Deissler and Boldman, 1974),

$$\frac{u}{w} = \frac{dr}{dz} = -\frac{1}{4}\frac{r}{z}$$

or

$$r/r_i = (z/z_i)^{-1/4} \tag{12}$$

where z_i is the value of z at some inner reference radius r_i. A plot of Eq. (12) is shown in Fig. 4, where w_0 is 0 and z increases negatively downward. This plot is not intended to imply that the velocities in a tornado are necessarily downward; the stream lines could just as well be plotted converging upward. However, in our experiments the vortex was heavier than the surrounding fluid, and its motion was downward.

In one experiment (Deissler and Boldman, 1974) the boiloff from liquid nitrogen, to which a small amount of initial vorticity was added, provided a source of cool, heavy gas which could accelerate downward to produce a concentration of vorticity. Condensation streamers made the flow visible.

Top and side views of the resulting gravity-driven vortex are shown in Fig. 5. The predicted stre.mline shown in Fig. 5(a) was calculated from (Deissler and Boldman, 1974)

$$\varphi = \varphi_i \frac{(r/r_0)^{-4} - 1}{(r_i/r_0)^{-4} - 1} \tag{13}$$

where the central angle φ was set equal to zero at an outer radius r_0 and φ_i is the value of φ at an inner radius r_i. Both the theory and the experiment show a characteristic hook shape for the streamlines. In the outer portion of the vortex the flow is nearly radial, whereas in the central portion it becomes nearly tangential.

It might be mentioned that the vorticity concentration shown in Fig. 5 was not dependent on having a flat surface immediately above the vortex. However a hollow cylinder several vortex diameters high and closed at the top was placed above the vortex to reduce the vertical velocity w_0 to a low value at the plane

where the fluid entered the vortex. According to Eq. (10), then, the radial velocity at that plane was large, and vorticity concentration could take place. In an actual tornado a temperature inversion (stable region above the vortex may have somewhat the same effect (Ward,1956). Similar results were obtained when a plate was placed immediately above the vortex. The plate simulates the ground if the upward and downward directions are reversed, so that the flow is thought of as being upward.

The side view of the vortex shown in Fig. 5(b) appears to be similar to that predicted in Fig. 4, at least for the region reasonably near the top. However to show the vertical development of the vortex somewhat more clearly, and to investigate the effect of vertical shear in the environment on the development of the vortex , we (Boldman and Deissler) devised another experiment, in which a rotating column of dyed dark corn syrup (specific gravity, 1.3) accelerated downward through horizontally flowing water. In this case the vertical velocity at the point where the heavy fluid entered the water was restricted to a comparatively low value by the friction in a rotating tube through which the fluid flowed before it entered the water.

Runs were made with and without rotation and with and without water flow. The results for the four cases are shown in Fig. 6. (In order to show the columns more clearly, the corn syrup lying on the bottom has been removed.) The contraction of the column as it accelerates downward to produce vorticity concentration (in the rotating cases) is clearly seen in this experiment, and is similar to that predicted in Fig. 4. The results with and without rotation appear to be about the same (except that the columns in the rotating cases whip around more). This result might be expected. if the analytical model in this section is applicable, since Eq. (5) or (7) is independent of rotation, and since the continuity condition for this case can be written as $D^2w = $ constant. Thus the diameter D of the column at any vertical position should be the same with rotation as without.

Comparison of the results with and without horizontal water flow (vertical wind shear) seems to show that the columns with water flow are somewhat smaller than those without. One might be inclined to expect this intuitively, since he night expect the vertical shear to cause additional stretching of the column. If, however, one modifies Eq. (5) for the case where the column makes an angle θ with the vertical, Eq. (5) becomes,

$$w \frac{dw}{dz} = -\beta g \left(T_{e0} - T + \frac{\partial T_e}{\partial Z} Z \right) \cos \theta \qquad (14)$$

where w and z are in the axial direction, and Z is in the vertical direction. But since $dZ = dz \cos \theta$, Eq. (14) becomes

$$w \frac{dw}{dZ} = -\beta g \left(T_{e0} - T + \frac{\partial T_e}{\partial Z} Z \right) \qquad (15)$$

which has the same form as the equation for $\theta = 0$ if w and Z are, respectively, in the axial and vertical directions. Since the continuity condition is still $D^2 w =$ constant, the column diameter with and without horizontal water flow should be the same at a particular vertical position. Therefore any differences between the cases with and without horizontal water flow in Fig. 6, if they are real, must be due to the effects of axial friction. Those effects were neglected in Eq. (15).

Thus, at least for these experiments, and with the possible exception of the effects of friction, the model considered in this section seems to be realistic. For a vortex-to-environment density ratio closer to one than the value of 1.3 in the experiment, as it probably is for a tornado, the axial drag may be relatively more important. The effects of drag, as well as several other effects, will be considered in the next section.

4. Effects Of Drag, Heat Transfer, And Precipitation-Induced Down Drafts

On The Axial Motion

We first estimate the axial drag on the vortex column. The axial turbulent shear stress on the column (molecular shear stress is negligible away from walls) is given by

$$\tau_0 = -\rho_a \overline{w'u'} = -\rho_a \frac{\overline{w'u'}}{(w - U \sin \theta)^2} (w - U \sin \theta)^2$$

$$= -\rho_a R(w - U \sin \theta)^2 \operatorname{sgn}(w - U \sin \theta) \tag{16}$$

where ρ_a is the air density, w' and u' are turbulent velocity components in the axial and radial directions, the overbar designates an averaged quantity, θ is the angle of inclination of the column with the vertical, w is the velocity of the column relative to a stationary point, and $U \sin \theta$ is the component of the horizontal wind velocity along the axis of the column. Thus the axial velocity of the column relative to the surrounding air is $w - U \sin \theta$. According to experiments of Liepman and Laufer for a free turbulent mixing layer (Townsend, 1956),

$$R \equiv \frac{|\overline{w'u'}|}{(w - U \sin \theta)^2} \sim 0.01 \tag{17}$$

The symbol sgn in Eq. (16) means sign of, and is included so that τ_0 will change sign if $w - U \sin \theta$ changes sign.

If rain drops are present in the column, they also exert a force if they move relative to the air in the column. The force of the drops acting on unit volume of air is

$$F_d = C_D \frac{\pi}{4} d^2 \frac{\rho_a n}{2} (w_d - w)^2 \operatorname{sgn}(w_d - w) \tag{18}$$

where C_D is the drag coefficient of the drops in the air, d is the drop diameter, w_d is the axial velocity of the drops relative to a stationary point, and n is the number of drops per unit volume.

If we write an axial force balance on a volume element of fluid of diameter D (including buoyancy, precipitation, and axial drag forces), where D is the column diameter at axial position z, we get, in place of Eq. (14),

$$\frac{dw^2}{dz} = -2\beta g \left(T_{e0} - T + \frac{\partial T_e}{\partial Z} Z \right) \cos\theta - \frac{\pi}{4} C_D d^2 \frac{(D^2 N)w}{w_d(D^2 w)} (w_d - w)^2 \operatorname{sgn}(w_d - w)$$

$$- \frac{8R}{|D^2 w|^{1/2}} |w|^{1/2} \left(w - \frac{\partial U}{\partial Z} Z \sin\theta \right)^2 \operatorname{sgn}\left(w - \frac{\partial U}{\partial Z} Z \sin\theta \right) \qquad (19)$$

where N is the number of drops passing through unit cross-sectional area of the column in unit time and is related to n in Eq. (18) by $N = nw_d$. Z is measured in the vertical direction, z in the axial direction. If drops are conserved, $D^2 N$ is constant for steady state. It has been assumed that the vertical wind gradient is constant, and that $U = 0$ for $Z = 0$. Thus U has been replaced by $Z \,\partial U/\partial Z$ in the last term in Eq. (19). By continuity, the quantity $D^2 w$ in Eq. (19) is a constant, since for realistic cases the cross sectional area of the drops is small compared with that of the column.

The first term on the right side of Eq. (19) gives the effect of buoyancy on the axial acceleration, the second term gives the effect of rain drops or hail, and the last term gives the effect of turbulent drag.

In order to get an equation for w_d, we write a force balance on a drop. This gives

$$\frac{dw_d^2}{dz} = -2g \cos\theta - \frac{3}{2} \frac{C_D}{d} \frac{\rho_a}{\rho_d} (w_d - w)^2 \operatorname{sgn}(w_d - w) \qquad (20)$$

where ρ_d is the density of the drop.

If heat transfer takes place between the column and the surroundings, the temperature T in the buoyancy term in Eq. (19) will vary with z. The turbulent heat transfer q_0 to the column per unit area can be related to the shear stress by a form of Reynolds analogy (Deissler, 1959):

$$q_0 = \frac{c_{pe}(T_e - T)|\tau_0|}{|w - (dU/dZ)\, Z \sin \theta|} \tag{21}$$

where c_{pe} is the effective specific heat in the column, and the quantity in the denominator is again the axial velocity of the column at z relative to the surrounding air. (We do not have to evaluate c_{pe}, since it drops out of the final equation.) Writing an energy balance on an element of fluid of diameter D, and using Eqs. (16) and (17) for the shear stress in Eq. (21), give

$$\frac{d(T_{e0} - T)}{dz} = \frac{4R}{|D^2 w|^{1/2}\, |w|^{1/2}} \left(T_{e0} - T + \frac{dT_e}{dZ} z \right) \left| w - \frac{dU}{dZ} Z \sin \theta \right| \tag{22}$$

Before calculations can be made, we still need a relation for θ, the local angle of the column with the vertical. In order to obtain such a relation, we assume that $U - u' = $ constant, where u' is the horizontal velocity of the column at z, so that $du'/dZ = dU/dZ$. Using that relation and the relation $u' = w \sin \theta$, we get

$$\frac{d(w^2 \theta)}{dz} = \frac{dU}{dZ} w + \left(\theta - \frac{1}{2} \tan \theta \right) \frac{dw^2}{dz} \tag{23}$$

from which θ can be obtained as $\theta = (w^2 \theta)/w^2$. The horizontal and vertical coordinates (X, Z) of the column at z are then given by

$$\frac{dX}{dz} = \sin \theta, \quad \frac{dZ}{dz} = \cos \theta \tag{24}$$

The diameter D of the column at z can be obtained from $D^2 = (D^2 w)/w$, where $D^2 w$ is a constant of the motion.

We can now solve the set of ordinary differential Eqs. (19), (20), and (22) to (24) numerically, if we know the initial conditions and the constants in the equations. For the initial conditions we set w, w_d, $T_{e0} - T$, $w^2 \theta$, X, and Z equal to 0 at $z = 0$. For the constants let $\beta = 1/330 \text{ K}^{-1}$, $g = 9.81 \text{ m/sec}^2$, $dT_e/dZ = -0.003 \text{ K/m}$,

$C_D = 0.4$ (for a solid sphere), $d = 0.001$ m, $R = 0.01$, $dU/dZ = 0.003$ sec^{-1}, and $\rho_a/\rho_d = 0.00086$. The potential temperatures and wind velocities correspond to average values given by Wills (1969) for tornado environments.

Calculated results for $D^2 w = -10^6$ and -10^7 are plotted in Figs. 7 and 8. For comparison, we note that the Dallas tornado had a $D^2 w \approx 4 \times 10^6$ (Hoecker, 1960). According to the results of Wills (1969), the effects of buoyancy and vertical wind shear in tornado-producing environments extend over the vertical distances shown. Values of $D^2 N$ of 10^8 and 10^9 in Figs. 7(a) and (b), respectively, with drop size $d = 0.001$ m, correspond to violent rain with some hail (Berry et al., 1945). However, results calculated for no rain agreed within a percent with those in Fig. 7. Thus the effect of rain in producing downdrafts in a tornado appears to be small compared with the effect of buoyancy for those values. However precipitation-induced downdrafts may be important for convecting large-scale vorticity downward at a slow rate in cases where buoyancy effects are small (Fugita, 1975). Calculations for no buoyancy but with the precipitation parameters the same as in Fig. 7 gave air-downdraft velocities of 0.5 m/sec with a drop velocity of about 7 m/sec at $Z = -6,000$ m. (In order to calculate nonzero velocities from Eqs. (19) and (20) for this case it was necessary to assume small initial values for w and w_d.) When the drop size was increased an order of magnitude to 0.01 m, a size which might occur for hail, downdraft velocities approached those for negative buoyancy (Fig. 8). Giant hail is in fact observed in connection with tornado occurrences (Browning, 1965). For this case it was even possible to obtain downdrafts with small positive buoyancy ($dT_e/dz = +0.0003$).

The contraction of the column as it is accelerated downward by buoyancy forces is clearly shown in Fig. 7, and is similar to that in the experiment in Fig. 6. The relative contraction for a given change in altitude is greater for the larger value of $D^2 w$ because the effects of axial drag and heat transfer are less for the larger column. As is the case for the drag, the effect of heat transfer is to decrease the

vertical acceleration. This latter decrease occurs because the buoyancy term in Eq. (19) is reduced by heat transfer to the column. The vertical wind shear deflects the column horizontally as it falls. It appears that the main effect of wind shear on the axial acceleration of the column is to decrease the axial drag term (last term in Eq. (19)). In no cases calculated was the effect of wind shear large enough to reverse the sign of the axial drag term.

Values of axial velocity are plotted against vertical position Z in Fig. 8. The results extend over a wider range of values of D^2w than those in Fig. 7. The smallest value of D^2w may be appropriate for dust devils as well as for small tornadoes. The axial velocities decrease as D^2w decreases because the restricting effects of drag and heat transfer are greater for the smaller columns, as discussed in the last paragraph. The curve for $D^2w = \infty$ is the same as that for no drag and heat transfer. Comparison of the solid with the dashed curve for $D^2w = 4\times10^6$ shows that the vertical wind shear increases the axial velocity at a given vertical position. This increase is due to the drag reduction produced by vertical shear (discussed in the preceding paragraph).

For the largest columns, the vertical velocities near the ground (if the ground is at $Z = -8,000$ m) approach tornadic values on the order of 70 m/sec. Even higher values would be obtained if the downdraft originated at higher altitudes, if the local potential temperature gradient were negatively greater than -0.003 (as it may well be), or if giant hail were present in large quantities. Thus aside from the effect of tangential velocities (to be investigated in the next section), it appears that buoyancy-induced downdrafts may be large enough to produce significant damage. This effect has been discussed by Rossman (1960). He presents a photograph by E. L. Van Tassel (U.S. Weather Bureau), shown in Fig. 9, which gives evidence of severe downdrafts in a tornado which passed through Bayard, Nebraska in 1951. Pieces of 2- by 8-inch boards were driven into the ground a depth of 18 inches. The ends driven into the ground were square (not splintered).

Fugita (1975) has also noted evidence of severe downdrafts in tornado environments. These observations appear to be consistent with the calculated results in Fig. 8 for the larger columns. Thus at least some of the damage produced by tornadoes appears to be due to downdrafts.

If we neglect the precipitation-drag term and let $T_{e0} - T = 0$ at $z = 0$ in Eq. (19), there is nothing in that equation which says that the motion should be either up or down; the buoyancy force in that case is zero at $z = 0$. Actually, from the observations and analyses of various authors, it appears that the velocities in some tornadoes (or parts of tornadoes) may be up, whereas in others it may be down (Rossman, 1960; Fugita, 1973, 1975; Davies-Jones et al., 1975; and Golden, 1975). Since Fig. 7 was for downflow, an upflow case ($D^2 w = 4 \times 10^6$) is plotted in Fig. 10. Most of the discussion for Fig. 7 applies also to this case.

As pointed out by Eskridge and Das (1976), and by Deissler and Boldman (1974), one difficulty with models which consider only updrafts is that the tornado would be expected to form before the rotating cloud forms, whereas the opposite is observed. As will be seen, there are probably regions of both updrafts and downdrafts in tornadoes.

5. Maintenance Of The Tangential Velocity

Except for a frictionless vortex model, the tangential velocity has not yet been considered. The effect of turbulent friction is important, in that it determines the maximum tangential velocity which can occur in a vortex; the maximum tangential velocity is often used as an indication of the violence of a tornado. Obviously the frictionless relation $v \propto r^{-1}$ cannot apply all the way to the vortex center.

In order to investigate the tangential velocity, we use Burgers' (1948) model for a steady-state viscous vortex, as modified for a turbulent viscosity by Deissler and Perlmutter (1960). The modified equation for the tangential velocity is

$$\frac{v}{v_0} = \frac{r_0}{r} \left\{ \frac{1 - \exp\left[(u_0/v_0)\, r^2 / \left(\kappa^2 r_0^2\right)\right]}{1 - \exp\left[(u_0/v_0)/\kappa^2\right]} \right\} \tag{25}$$

where u_0 and v_0 are respectively the radial and tangential velocities at an outer vortex radius r_0, and κ is the Kárman constant. For most of the cases considered here, the flow is radially inward (u_0 is negative). By continuity, when a radial flow is present, there must also be an axial flow. In deriving Eq. (25), we let w vary with z only ($w \propto z$), and $u/u_0 = r/r_0$. These relations (including Eq. (25)) satisfy the equations of motion and continuity. The outer vortex radius r_0 can be considered as the radius where w in an actual vortex begins to fall off rapidly with increasing r. The molecular kinematic viscosity was replaced by a turbulent viscosity ϵ, and ϵ was obtained from a modified form of von Kárman's similarity hypothesis as (Deissler and Perlmutter, 1960)

$$\epsilon = \kappa^2 v_0 r_0 / 2 \tag{26}$$

where v was taken proportional to r^{-1}, as it is for the outer portion of the vortex. The constant value for ϵ given by Eq. (26) was assumed to apply to the whole vortex, since the turbulence (at least for most of the cases of interest) is convected from the outer regions to the center of the vortex by the radial inflow. Strictly speaking, Eq. (25) applies only to the case where u and v are independent of z. However, outside of the regions of steep gradients in a boundary layer, Eq. (25) should be sufficiently accurate for the purposes for which it is used here. In Deissler and Perlmutter it was found that for confined vortex flows, the Kárman constant $\kappa \approx 0.3$. That value of κ was also found to be reasonable for the experiments of Wan and Chang (1972) for a tornado-like

vortex in the region above the surface boundary layer. Thus the value of $\kappa = 0.3$ is retained here.

A plot of Eq. (25) is given in Fig. 11. In the outer region of the vortex, $v \propto r^{-1}$, whereas for small r, $v \propto r$. As $-u_0$ increases, the region for $v \propto r^{-1}$ extends to smaller r, so that the maximum tangential velocity increases (for a given v_0). Thus for large tangential velocities, large radial inflows are required. For a comparison a case where the radial flow is outward ($u_0/v_0 = 1$) is also shown. The tangential velocities are small except at large radii. This kind of velocity distribution may occur in rotating clouds, where the flow may be outward (Hsu and Fattahi, 1975).

We want to relate the maximum tangential velocity v_m to the radial-inflow velocity u_m at the same point. To that end set dv/dr from Eq. (25) equal to zero. Then let $u_0 = u_m r_0/r_m$, since (according to our model) u varies linearly with r, and let $r = r_m$, the radius at which v is a maximum. This gives

$$\left(1 - \frac{2}{\kappa^2}\frac{u_m}{v_m}\frac{v_m r_m}{v_0 r_0}\right)\exp\left(\frac{1}{\kappa^2}\frac{u_m}{v_m}\frac{v_m r_m}{v_0 r_0}\right) - 1 = 0$$

Equation (25) becomes, for $r = r_m$ and $u_0 = u_m r_0/r_m$,

$$\frac{v_m r_m}{v_0 r_0} = \frac{1 - \exp\left[(1/\kappa^2)(v_m r_m/v_0 r_0)(u_m/v_m)\right]}{1 - \exp\left[(1/\kappa^2)(v_m r_m/v_0 r_0)(u_m/v_m)(r_0/r_m)^2\right]}$$

For large r_0/r_m (greater than about 2.5, which will occur if $v \propto r^{-1}$ near r_0) these two equations give, with $\kappa = 0.3$,

$$v_m r_m/v_0 r_0 = 0.72$$

and

$$u_m/v_m = -0.155 \tag{27}$$

This remarkably simple relation allows us to estimate the radial-inflow velocity required to maintain a given maximum tangential velocity. Thus v_m for the Dallas tornado is given by Hoecker (1960) as about 70 m/sec at a radius r_m of about 70 m. These values, or values slightly higher. probably apply also to the Cleveland tornado (Lewis and Perkins, 1953). Thus from Eq. (27) $u_m \approx -10.8$ m/sec.

We now ask whether a buoyancy-induced sink is large enough to produce this required va'ue of radial inflow velocity. For no axial friction and no heat transfer to the column (these factors would tend to decrease u_m), and for $T_{e0} - T = 0$ at $z = 0$, and $w_0 = 0$ (or for large z), Eq. (9) gives, for Will's tornado-environment data and for the Dallas tornado, $u_m \approx 0.33$ m/sec. This is smaller than the above value of u_m required to produce the observed tangential velocity by a factor of about 33. Thus it appears that buoyancy effects far from any restriction of vertical-flow velocity (large z) are much too small to sustain the tangential velocities observed in typical tornadoes. According to Eqs. (9) and (27) the potential temperature gradient would have to be about $(33)^2$ times as great as the average value observed for tornado occurrences. However for very large vortices, with r_m on the order of a mile or more (large for a tornado), Eqs. (9) and (27) show that tangential velocities of tornadic magnitude might be maintained by buoyancy forces in regions away from vertical-flow restrictions.

One possibility we should investigate is that the large tangential velocities in tornadoes may be produced transiently, say by random turbulence effects. (In a random distribution some eddies will be very strong.) In that case we can estimate the order of magnitude of the decay time t_d (with small radial flow) from the unsteady equation for the tangential velocity (Goldstein, 1938) as

$$\frac{\partial v}{\partial t} \sim \frac{v_m}{t_d} \sim \epsilon \frac{v_m}{r_m^2} \sim \frac{\kappa^2}{2} v_m r_m \frac{v_m}{r_m^2}$$

or

$$t_d \sim \frac{2}{\kappa^2} \frac{r_m}{v_m} \tag{28}$$

where the kinematic viscosity was replaced by a turbulent viscosity ϵ given by Eq. (26). For the Dallas tornado $t_d \sim 20$ sec, a time which, although longer than that obtained earlier by simply considering the vortex as a turbulent eddy, is still too short for a tornado. (Average tornado lifetime is about 13 minutes (Eskridge and Das, 1976).)

Thus it appears that the tangential velocity in tornadoes must be maintained by radial-inflow velocities on the order of those given by Eq. (27). But the values given by Eq. (9) for regions away from vertical-flow restrictions, are much too small. Equation (10) shows, however, that for regions where w_0 is small, as above a surface (for upflow), or beneath a stable inversion (for downflow), u can be large if $T_{e0} - T$ is nonzero at $z = 0$. Thus we let $w_0 = 0$ and $T_{e0} - T = 0$, -2 and -4 K, and $r = r_m = 70$ m in Eq. (8).

The resulting curves for u_m are plotted against z in Fig. 12. The large effect of $T_{e0} - T$ near $z = 0$ is evident. At least for a few meters above the surface (or beneath an inversion), the values of u_m are of the right order of magnitude to maintain the tangential velocities observed in tornadoes, according to Eq. (27). Thus a vortex potential temperature which is a few degrees different from the surroundings in a region where the vertical velocities are restricted to low values appears to be necessary for maintaining the vortex by buoyancy forces. Conditions particularly favorable for this type of vortex maintenance should occur for fire whirls (and possibly for dust devils) where high local surface temperatures are prevalent (high $T_{e0} - T_0$). Of course, in those cases, the smallness of r in Eq. (8) would tend to work against maintenance by buoyancy.

This section has emphasized the tangential velocity (maintained by the radial inflow) as the destructive element in tornadoes. According to Eq. (27) the radial

velocity is only about 15 percent of the tangential velocity at the radius where the tangential velocity is a maximum. However, the ratio $u_0/v_m = (u_0/v_0)(v_0/v_m)$ varies from 0.5 to 1.3 for the values of u_0/v_0 in Fig. 11. Thus the radial velocity in the outer part of the vortex can be of the same order of magnitude as the maximum tangential velocity. This appears to be the case for the experiment in Fig. 5a, where the streamlines are nearly radial in the outer part of the vortex.

According to Eq. (8), u becomes infinitely large at a surface where $z = 0$, $w_0 = 0$, and $T_{e0} - T \neq 0$. In reality, of course, u decreases in a thin boundary layer above the ground and goes to zero at the ground. The important subject of the surface boundary layer will be considered in the next section. As will be seen, the surface boundary layer can have a large effect on the radial inflow, even when buoyancy effects near the surface are small.

6. The Surface Boundary Layer

The surface boundary layer below a vortex has been studied analytically by Kuo (1971), Lewellen (1962), and others; and experimentally by, for instance, Chang (1969), Wan and Chang (1972), and Savino and Keshock (1965). According to the physical picture usually given, the centrifugal force produced by the rotating flow is in approximate equilibrium with the radial pressure gradient in the region above the boundary layer. Within the boundary layer the centrifugal force is reduced because v is smaller there. If the pressure is approximately constant across the boundary layer, so that the radial pressure gradient does not change appreciably, there will be a net inward force in the boundary layer which tends to produce large radial inflows there. These radial inflows (given by Eq. (27)) may be large enough to maintain the tangential velocities observed in tornadoes. The intensification of the vortex by the presence of the boundary layer has been shown by Hsu and Tattahi (1975), who ran experiments both with and without a ground plate (no buoyancy). Waterspouts, which travel over water, may not be as violent as tornadoes, which travel over land, because the tangential velocity

probably does not go to zero at the surface of the water, as it does at a land surface.

After the fluid leaves the boundary layer vertically, it will continue upward if the local buoyancy force is large enough (see preceding section). Otherwise at least part of it will tend to recirculate, as in the experiments of Wan and Chang (1972) (Fig. 13). It is of interest that in those experiments the airflow in the outer part of the vortex was downward, even though the air entered the apparatus radially from a location below the ground plate and exhausted through the ceiling. This recirculation will no doubt take place in a tornado unless the potential temperature in the vortex at the ground is several degrees higher than that in the surroundings, as in Fig. 12. There is some evidence that air descends from a rotating parent cloud at large radii (as a collar cloud) and then travels radially inward in the surface boundary layer (e.g., the Xenia tornado (Fugita, 1975)). Eskridge and Das (1976) have indicatated that precipitation-induced downdrafts surrounding tornadoes may be warm. In that case the air at the surface which enters the tornado updraft may have a potential temperature several degrees higher than that of the surroundings, so that according to Fig. 12 and Eq. (8), radial inflows sufficiently large to produce tangential velocities of tornadic magnitude (Eq. (27)) may be produced by buoyancy forces. Although this is an appealing suggestion, its occurrence will depend on the presence of positive buoyancy, and on precipitation drops of sufficient size and density to bring down the warm air. A sample calculation using Eqs. (19) to (24) showed that with the conditions for the precipitation case in Fig. 8 (dot-dashed curve), but with positive buoyancy ($dT/dZ = +0.0003$), air which descended 8,000 m to a surface because of falling precipitation was about 1.3 K warmer than the surroundings at the surface. Its downdraft velocity near the surface was about 40 m/sec. If, on the other hand, the air descending at large radii is cool, it will have to be pushed up mechanically at smaller radii.

In cases where the buoyancy forces are small, what is the source of energy for the tornado? Apparently it is the rotating parent cloud above the vortex. Thus the rotating cloud centrifuges air outward which then descends, swirling at large radii. At the surface at least part of the air becomes trapped in the boundary layer, where it spirals inward, and then upward, to form the vortex (Fugita, 1975; Hsu and Fattahi, 1975; Hsu, 1973; and Szillinsky and Wipperman, 1969). (This is somewhat similar to the stirred teacup effect.) Experimental flow patterns obtained by Hsu and Fattahi (1975) for a rotating honeycomb above a surface are shown in Fig. 14. Note that the vortex produced at the surface is off-center; it follows a circular path around the centerline of the apparatus.

There is also recent evidence (e.g., the Xenia tornado (Fugita, 1975)) that considerable damage is done by small, intense short lived vortices, called suction vortices, which drop to the ground from the larger vortex. The surface layer probably also has an important effect on the dynamics of these smaller vortices.

Next we estimate the thickness δ of the friction layer where u goes from zero at the ground to its maximum value. Above that point u again decreases. Calculated values for δ, using tangential velocities and radii for tornadoes, should at least show whether such conditions are likely to occur for a boundary layer.

The equation for the boundary layer for the radial flow is

$$u \frac{\partial u}{\partial r} + w \frac{\partial u}{\partial z} - \frac{v_b^2}{r} = -\frac{1}{\rho} \frac{\partial p}{\partial r} + \frac{1}{\rho r} \frac{\partial}{\partial z}(r\tau) \tag{29}$$

where p is the pressure, τ is the shear stress, and v_b is a value of v in the friction layer. At some distance outside the friction layer for u the centrifugal force term will be in approximate equilibrium with the pressure-gradient term, or

$$\frac{v^2}{r} \approx \frac{1}{\rho} \frac{\partial p}{\partial r} \tag{30}$$

An assumption generally made in analyses of vortex boundary layers is that the pressure is constant from the wall to the distance where Eq. (30) applies. We will retain that assumption, although the data of Wan and Chang (1972) indicate that it is only approximately constant. Also, the thickness of the friction layer where u goes from zero to its maximum value is small compared with the thickness of the boundary layer for v (Wan and Chang, 1972), so that $v_b \ll u$ in Eq. (29). Equation (29) becomes, with Eq. (30),

$$u \frac{\partial u}{\partial r} + w \frac{\partial u}{\partial z} = -\frac{v^2}{r} + \frac{1}{\rho r} \frac{\partial (r\tau)}{\partial z} \tag{31}$$

where v is measured outside the boundary layer, where Eq. (30) applies. The first term on the right side of Eq. (31) accelerates the fluid radially inward in the friction layer. In the remainder of the analysis we consider quantities at r_m, the radius where v outside the boundary layer is a maximum, v_m. At that radius $\partial u/\partial r \approx u_m/r_m$. Moreover w varies linearly with z for small z. Also, since the boundary layer is turbulent, the velocity u parallel to the surface can be approximated by $-u \propto z^{1/7}$. By introducing these approximations into Eq. (31) and integrating from the wall to $z = \delta_m$, where $-u$ is a maximum and $\tau = 0$, we get

$$\frac{7}{9} u_m^2 \frac{\delta_m}{r_m} + \frac{1}{8} u_m w_m = -\frac{v_m^2}{r_m} \delta_m + \frac{\tau_w}{\rho} \tag{32}$$

where τ_w, the shear stress at the wall, can be approximated by the Blassius relation

$$\frac{\tau_w}{\rho} = 0.0228 \, u_m^2 \left(\frac{\nu}{-u_m \delta_m} \right)^{1/4} \tag{33}$$

where ν is the kinematic viscosity. By performing the same operations on the continuity Eq. (1), we get

$$w_m = -\frac{7}{4} u_m \frac{\delta_m}{r_m} \tag{34}$$

From Eqs. (32) to (34) we have

$$\delta_m = \left[\frac{0.0228 \ r_m}{0.559 + (-u_m/v_m)^2}\right]^{4/5} \left[\frac{\nu}{(-u_m/v_m)v_m}\right]^{1/5} \tag{35}$$

The ratio $-u_m/v_m$ in Eq. (35) is measured at $z = \delta_m$, whereas that in Eq. (27) is measured near the edge of the boundary layer for v. Since the value of δ_m calculated from Eq. (35) is somewhat insensitive to u_m/v_m, it should be sufficiently accurate for our purpose to use the value from Eq. (27). Setting $-u_m/v_m = 0.155$ gives

$$\delta_m = 0.11 \left(\nu r_m^4/v_m\right)^{1/5} \tag{36}$$

Note that the surface boundary layer is the only part of a tornado where the kinematic viscosity ν is not negligible compared with the turbulent viscosity.

For Case 2 in Wan and Chang's (1972) experiment (Case 2 has features similar to those of a tornado), their Table 1 gives $r_m = 0.076$ m and $v_m = 19.8$ m/sec. With $\nu = 1.5 \times 10^{-5}$ m^2/sec, Eq. (36) gives $\delta_m/r_m = 0.011$, a value that appears consistent with results in Wan and Chang's Fig. 12. Similarly for the Dallas tornado, where $r_m \approx 70$ m and $v_m \approx 70$ m/sec (Hoecker. 1960) we get $\delta_m = 0.16$ m. This value, although small compared with the other lengths in the tornado is, according to Eq. (36), large enough to maintain the tangential velocity by radial inflow. Although $-u$ quickly reaches a maximum as z increases to δ_m, its decrease with further increases of z is, according to the experiment of Wan and Chang, much more gradual. Thus, the radial velocities in the boundary layer should be high enough to maintain tangential velocities of tornadic magnitude for some distance above the ground. Equation (33) is for a smooth surface. For a rough terrain δ_m would be larger than the value given by Eq. (36).

7. Summary And Conclusions

Although we have not been able to obtain a single model applicable to all tornadoes it may be that there is, in fact, no unique mechanism for all tornadoes. We have pointed out probable ways the strong vortices may originate and persist, as well as how they may be structured. These suggestions were supported, as much as possible, by calculations and observations.

Random vortices were shown to grow with time in an atmosphere with buoyant instability and vertical wind shear. Thus if those conditions persist long enough, the occurrence of strong atmospheric vortices becomes highly probable. The analysis showed that strong radial inflows must occur in the vortices, if their high tangential velocities are to be maintained for a reasonable length of time.

A relation between the maximum tangential velocity in a tornado and the radial-inflow velocity at the same radius (Eq. (27)) was obtained from a turbulent-vortex model. The radial velocity was found to be roughly 15 percent of the tangential velocity at the radius where the tangential velocity is a maximum. It was shown that tangential velocities of tornadic magnitude could be maintained by buoyancy-induced radial inflows. However, it would be necessary for the potential temperature in the vortex to differ from that of the surroundings by several degrees at a point where the vertical velocity is small or zero (at the ground surface or below a stable inversion). Buoyancy effects in regions away from surfaces or stable layers were too small to maintain large tangential velocities, except for very large vortices with radii for the maximum tangential velocity on the order of a mile or more (large for a tornado).

If buoyancy effects are small, the boundary layer next to the ground (where centrifugal effects are reduced) must be relied on to allow the large radial inflows required to maintain the vortex. The thickness of the friction layer where the radial velocity goes from zero to a maximum as height increases, was found to be extremely thin (less than a meter) for a smooth surface. For a rough terrain the thickness would be greater.

A physical picture which seems to emerge, and which may be applicable to many tornadoes is the following: A large vortex or rotating cloud (turbulent eddy) is produced, possibly by the effects of buoyancy and vertical shear, as discussed in section 2. The rotation of the parent cloud tends to centrifuge air in the outward direction. The rotating air then descends at large radii because of the vertical circulation pattern set up by the rotating cloud. This descent may be aided by negative buoyancy effects and precipitation, if the potential temperature at the cloud is lower than that at the surface. If, on the other hand, the potential temperature at the cloud is higher than that at the ground, buoyancy will tend to retard the descent at large radii but the air may still descend because of precipitation and the natural vertical circulation pattern set up by the rotating cloud.

As the rotating air reaches the ground, at least part of it will be trapped in the surface boundary layer and will flow inward at high radial velocities (high enough to produce tangential velocities of tornadic magnitude). This radial inflow is caused by the reduced centrifugal force in the boundary layer and, if the air is warmer than the surroundings (if it came from a warm cloud), will be aided by the buoyancy sink produced by rising air at small radii. If, on the other hand, the air is cooler than the surroundings, the radial inflow will be hindered. The air will flow upward at small radii because of the natural circulation pattern set up by the rotating cloud and, if the air is warm, because of buoyancy forces. Of course if the air is cool, its upward flow will be hindered. As the air reaches the cloud level, the cycle may be repeated. The tornado would be expected to last as long as the rotation of the cloud continues to be sufficiently large and/or buoyancy and precipitation forces continue to be effective.

According to this model a tornado might be produced regardless of which way the buoyancy forces act. The essential ingredient seems to be the rotation of the cloud. Precipitation at large radii should also have a positive effect regardless of the direction of buoyancy forces. The small intense suction vortices observed in tornadoes may also have essentially the mechanism outlined here.

Although much of the damage done by tornadoes is probably caused by their high tangential velocities, calculations and observations show that downdraft velocities in negatively buoyant columns can reach tornadic magnitudes. The analytical model, which was supported by laboratory experiments, took into account the effects of buoyancy, axial drag, heat transfer, and precipitation flow. Both axial drag and heat transfer tended to reduce the downdraft and updraft velocities significantly. (They had stabilizing effects.) When buoyancy was present, precipitation had a comparatively negligible effect when values of drop flux and size for violent rain were used. However when buoyancy effects were absent, the precipitation caused the column to still descend at a low velocity. When drop sizes an order of magnitude higher were used (1 cm), as might occur for hail, the downdraft velocities produced by precipitation flow approach those produced by buoyancy.

The results also showed that radial-inflow velocities in the outer part of a vortex may be comparable to the maximum tangential velocities. Although the radial inflows and downdrafts in a tornado may cause considerable destruction, the destruction associated with the tangential velocities may be still greater, because of the low central pressures which accompany the tangential velocities.

Acknowledgment

References

Beers, N. R., 1945: Numerical and graphical data. Handbook of Meteorology, F. A. Berry, E. Bollay, and N. R. Beers, eds., McGraw-Hill, 114.

Browning, K. A., 1965: The evolution of tornadic storms. J. Atm. Sci. 22, 664-668.

Burgers, J. M., 1948: A mathematical model illustrating the theory of turbulence. Advances in Applied Mechanics, vol. 1. R. von Mises and T. von Kármán, eds., Academic Press, Inc., 198.

Chang, C. C., 1969: Recent laboratory model study of tornadoes. Preprints Sixth Conference on Severe Local Storms, Amer. Meteor. Soc., 244–252.

Davies-Jones, R. P., Burgess, D. W., and Lemon, L. R., 1975: Analysis of the 4 June 1973 Normal Tornadic Storm. Preprints, Ninth Conference on Severe Local Storms, Amer. Meteor. Soc., 384–387.

Deissler, R. G., 1959: Turbulent heat transfer and friction in smooth passages. Turbulent Flows and Heat Transfer, C. C. Lin, ed., Princeton Univ. Press, 290.

Deissler, R. G. and M. Perlmutter, 1960: Analysis of the flow and energy separation in a turbulent vortex. Int. J. Heat Mass Transfer 1, 173–191.

Deissler, R. G., 1967: Effects of combined buoyancy and shear on weak homogeneous turbulence. NASA TN D-3999.

Deissler, R. G., 1971: Growth due to buoyancy of weak nomogeneous turbulence with shear. Z. Angewandte Math. Phys. 22, 267–274.

Deissler, R. G. and D. R. Boldman, 1974: Tornadolike Gravity-driven vortex model. NASA TN D-7738.

Eskridge, R. E. and P. Das, 1976: Effect of a precipitation-driven downdraft on a rotating wind field: a possible trigger mechanism for tornadoes? J. Atmos. Sci. 33, 70–84.

Fugita, T. T., 1960: Cumulus Dynamics, C. E. Anderson ed., Pergamon Press, New York, pp. 175-177.

Fugita, T. T., and H. Grandoso, 1968: Split of a thunderstorm into anticyclonic and cyclonic storms and their motion as determined from numerical model experiments. J. Atmos. Sci. 25, 416-439.

Fugita, T. T., 1973: Proposed mechanism of tornado-formation from rotating thunderstorm. Preprints, Eighth Conf. on Severe Local Storms. Denver, Colo., Amer. Meteor. Soc., 191-196.

Fugita, T. T., 1975: New evidence from April 3-4, 1974 tornadoes. Preprints, Ninth Conference on Severe Local Storms, Amer. Meteor. Soc., 248-263.

Golden, J. H., and D. Purcele, 1975: Photogrammetric velocities for the Great Bend, Kansas tornado: accelerations and asymmetries. Preprints, Ninth Conference on Severe Local Storms, Amer. Meteor. Soc., 336-343.

Goldstein, S., ed., 1938: Modern Developments in Fluid Dynamics. Vol. 1, Oxford Univ. Press, 104.

Hoecker, W. H., Jr., 1960: Wind speed and airflow patterns in the Dalls tornado of April 2, 1957. Mon. Wea. Rev., 88, 167-180.

Hoecker, W. H., Jr., 1961: Three-dimensional pressure pattern of the Dallas tornado and some resulting implications. Mon. Wea. Rev., 89, 533-542.

Hsu, C. T., 1973: Laboratory modelling of the tornado suction mechanism. Preprints, Eighth Conf. on Severe Local Storms, Amer. Meteor Soc., 199-202.

Hsu, C. T., and B. Fattahi, 1975: Tornado funnel formation from a tornado cyclone. Preprints, Ninth Conf. on Severe Local Storms, Amer. Meteor. Soc., 358-363.

Isaacs, J. D., et al., 1975: Effect of vorticity polution by motor vehicles on tornadoes. Nature 253, 254-255.

Kuo, H. L., 1966: On the dynamics of convective atmospheric vortices. J. Atmos. Sci., 23, 25-42.

Kuo, H. L., 1971: Axisymmetric Flows in the boundary layer of a maintained vortex. J. Atmos. Sci., 28, 20-41.

Landau, L. D., and E. M. Lifshitz, 1959: Fluid Mechanics, Pergamon Press, New York, p. 212.

Lewellen, W. S., 1962: A solution for three-dimensional vortex flows with strong circulation. J. Fluid Mech., 14, 420-432.

Lewis, W., and P. J. Perkins, 1953: Recorded pressure distribution in the outer portion of a tornado vortex. Mon. Wea. Rev. 81, 379-385.

Manton, M. J., 1976: Tornado forum. Nature, 260, 458

Modahl, A. C., and W. M. Gray, 1971: Summary of funnel cloud occurrences and comparison with tornadoes. Mon. Wea. Rev. 99, 877-882.

Preprints, Ninth Conf. of Severe Local Storms, 1975, Amer. Meteor. Soc.

Rossman, F. O., 1960: Cumulus Dynamics, C. E. Anderson ed., Pergamon Press, New York, 167-174.

Savino, J. M., and E. G. Keshock, 1965: Experimental profiles of velocity components and radial pressure distributions in a vortex contained in a short cylindrical chamber. NASA TN D-3072.

Science, 1972: 176, cover.

Szillinsky, A., and F. Wippermann, 1969: The penetration of tornado-like vortices into the boundary layer: numerical experiments. AFCRL-69-0321, Air Force Cambridge Research Lab.

Townsend, A. A., 1956: The structure of turbulent shear flow. Cambridge Univ. Press, 179.

Wan, C. A., and Chang, C. C, 1972: Measurements of the velocity in a simulated tornado-like vortex using a three-dimensional velocity probe. J. Atm. Sci., 29, 116-127.

Ward, N. B., 1956: Temperature inversion as a factor in formation of tornadoes. Bull. Amer. Meteor. Soc., 37, 145-151.

Wills, T. G., 1969: Characteristics of the tornado environment as deduced from proximity soundings. Paper No. 140, Dept. of Atmos. Sci., Colorado State Univ.

Figure 1. - First tornado cloud known to have been photographed (Miner County, South Dakota, August, 1884).
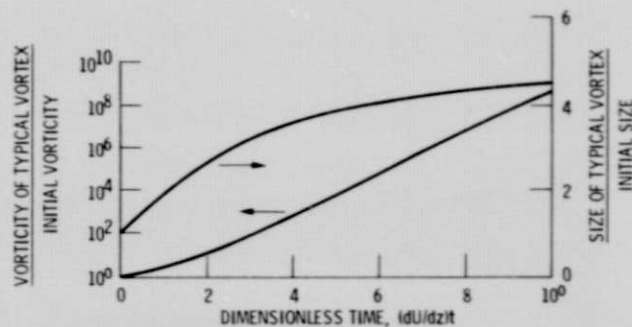
Figure 2. - Growth with time of vorticity and size of typical random vortex in an unstable atmosphere with vertical wind shear. Richardson number $= \beta g (dT/dz)/(dU/dz)^2 = -10$. Characteristic initial dimensionless wavenumber $\kappa_0^\circ = \nu^{1/2} \kappa_0/(dU/dz)^{1/2} = 2$.
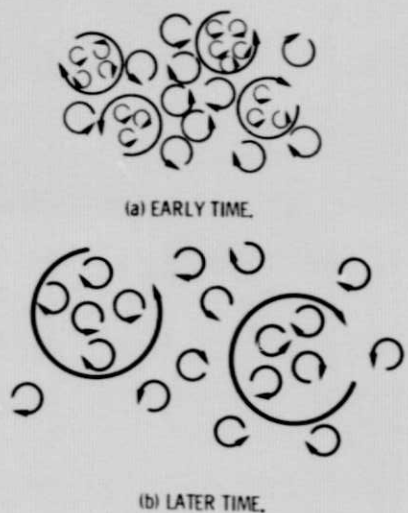

(a) EARLY TIME.

(b) LATER TIME.

Figure 3. - Growth of vortices in an unstable atmosphere with vertical shear. Heavier lines indicate stronger vortices.
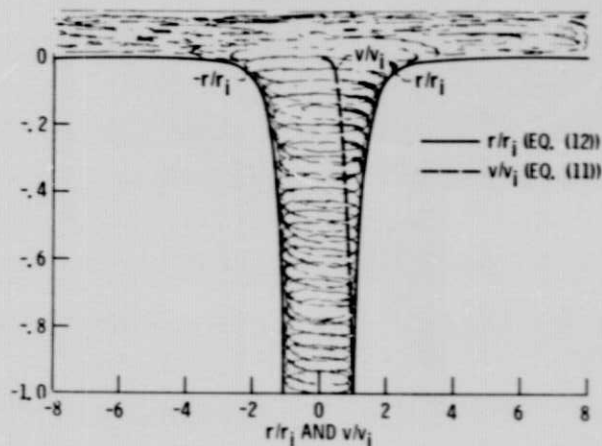
Figure 4. - Predicted variations, with vertical distance, of radius and tangential velocity along a streamline for a frictionless adiabatic model.
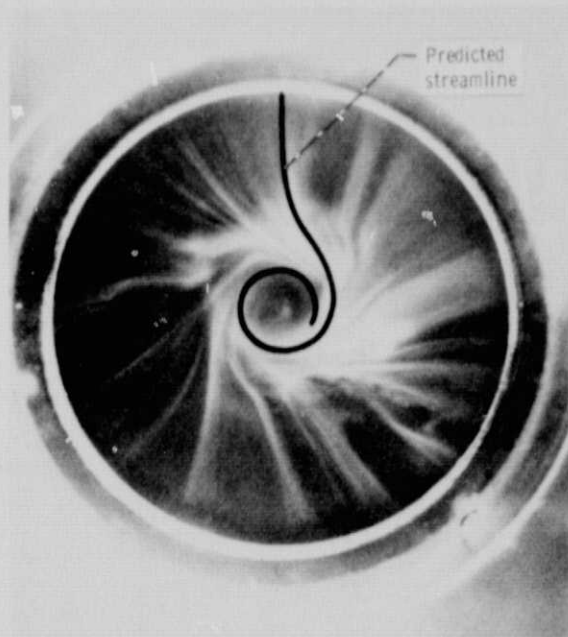
(a) Top view. Comparison of calculated streamline (Eq. (13)) with experiment.

(b) Side view.

Figure 5. - Gravity driven vortex (Deissler and Boldman (1974)).
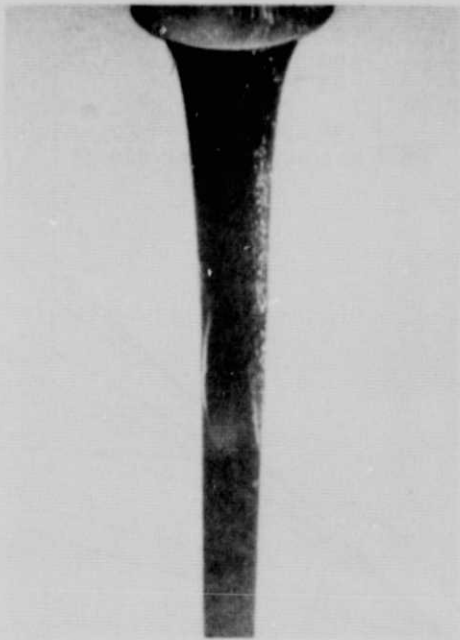
(a) Column not rotating. No horizontal water flow.
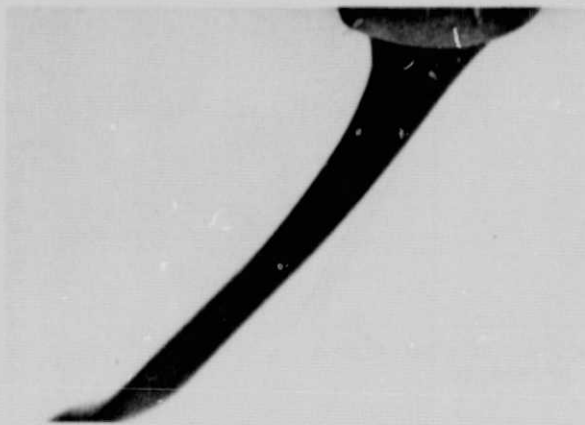
(b) Column not rotating. Water flowing horizontally (25.4 cm-sec^{-1}).
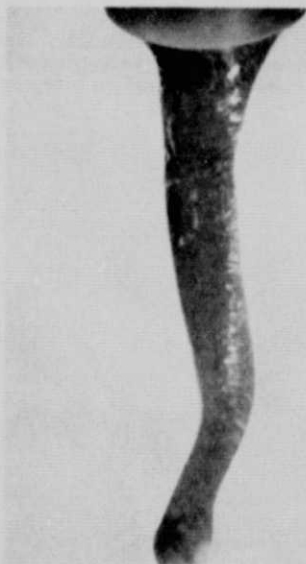
(c) Column rotating (tube above column rotating at 2.3 rps). No horizontal water flow.

(d) Column rotating (tube above column rotating at 2.3 rps). Water flowing horizontally (25.4 cm-sec^{-1}).

Figure 6. - Photographs showing downward acceleration of a column of heavy liquid (specific gravity · 1.3) in water.

(a) $D^2 w = -10^6$ m^3/SEC, $D^2 N = 0$, 10^8 DROPS/SEC.

(b) $D^2 w = -10^7$ m^3/SEC, $D^2 N = 0$, 10^9 DROPS/SEC.
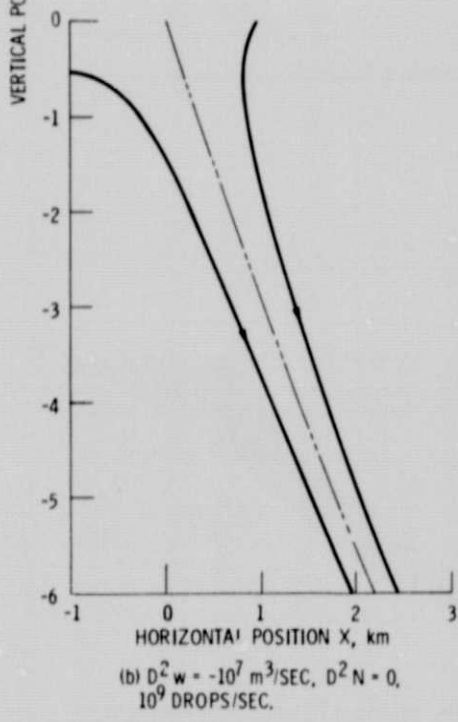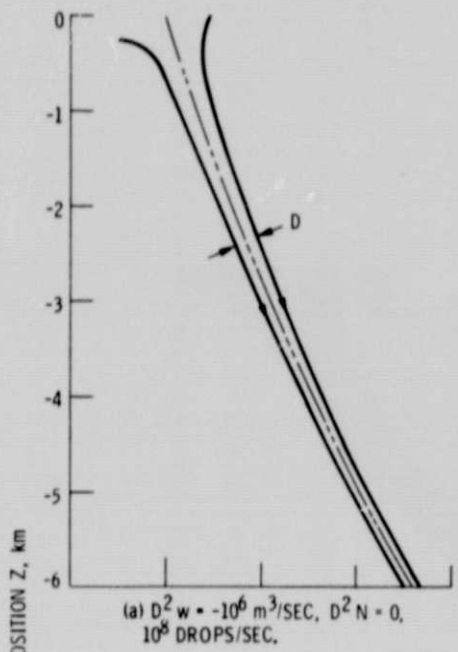
Figure 7. - Plots showing contraction of column accelerating downward with negative buoyancy, vertical wind shear, and precipitation. $dT/dZ = -0.003^0$ K-m^{-1}, $dU/dZ = 0.003$ sec^{-1}, initial $T_e - T = 0$. Drop size $d = 0.001$ m. Diameter D is to same scale as other distances.
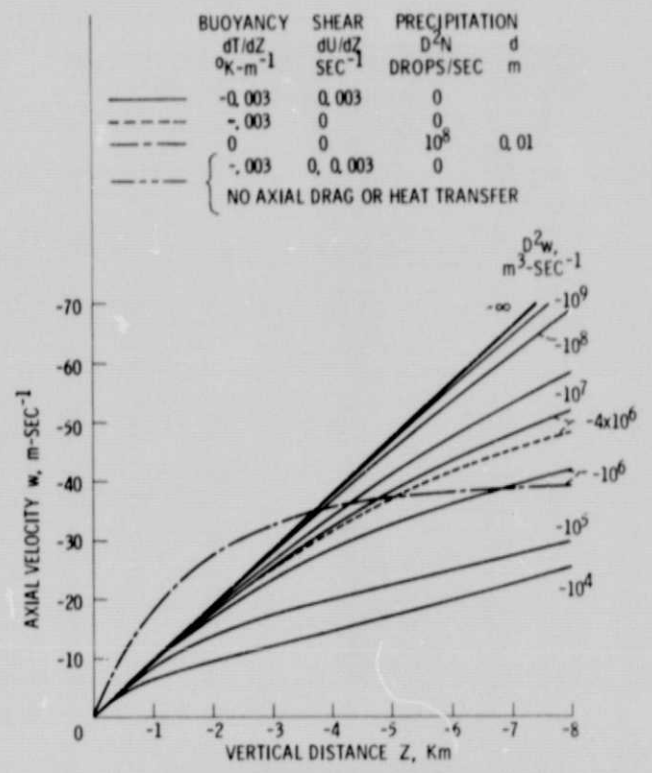

BUOYANCY	SHEAR	PRECIPITATION	
dT/dZ	dU/dZ	D^{2}N	d
^{0}K-m^{-1}	SEC^{-1}	DROPS/SEC	m
-0.003	0.003	0	
-.003	0	0	
0	0	10^8	0.01
-.003	0, 0.003	0	

NO AXIAL DRAG OR HEAT TRANSFER

Figure 8. - Variation of axial velocity with vertical position, D^{2}w, potential temperature gradient, vertical wind shear, and precipitation. Other quantities same as in figure 7.

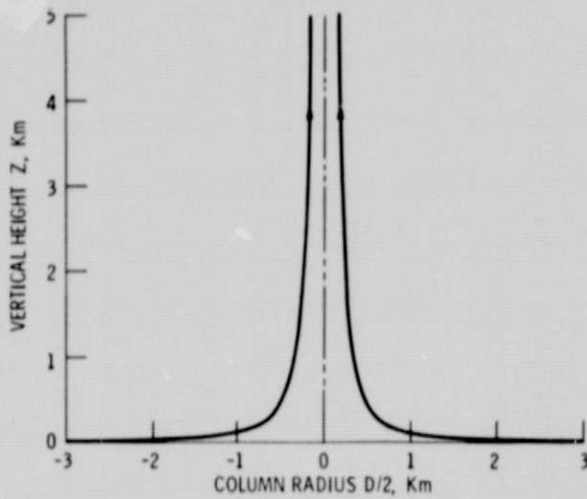Figure 9. - Evidence of severe downdraft (photograph taken by E. L. Van Tassel, U. S. Weather Bureau).

E-2213

Figure 10. - Plot showing contraction of column accelerating upward with buoyancy. $D^2 w = 4 \times 10^6$, $dU/dZ = 0$. No precipitation. Other quantities same as in figure 7.
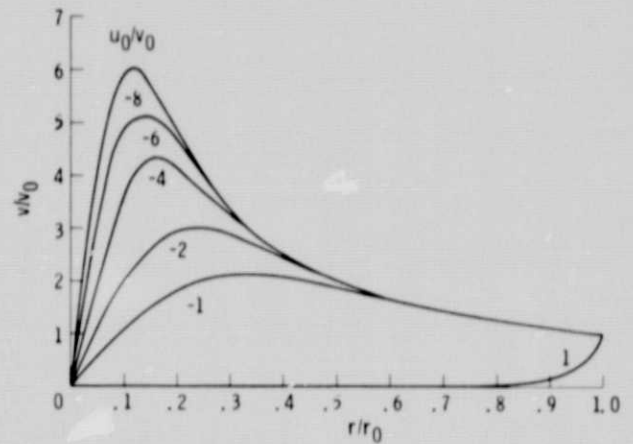

Figure 11. - Variation of tangential velocity with radius and radial velocity. Subscripts 0 indicate values at an outer reference radius r_0.
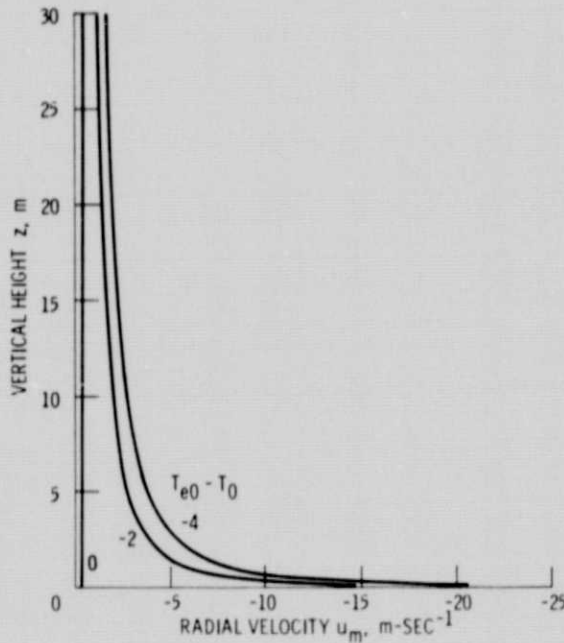

Figure 12. - Variation of radial-inflow velocity u_m (at r_m, where v is a maximum) with vertical height and temperature difference at $z = 0$, as calculated from Eq. (8). $w_0 = 0$, $dT_e/dz = -0.003$, $r_m = 70$ m.
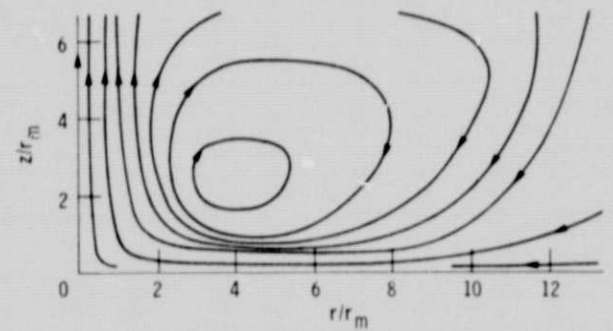

Figure 13. - Plot showing recirculation currents in experiment of Wan and Chang (1972) (case 2). r_m is radius where tangential velocity is a maximum.
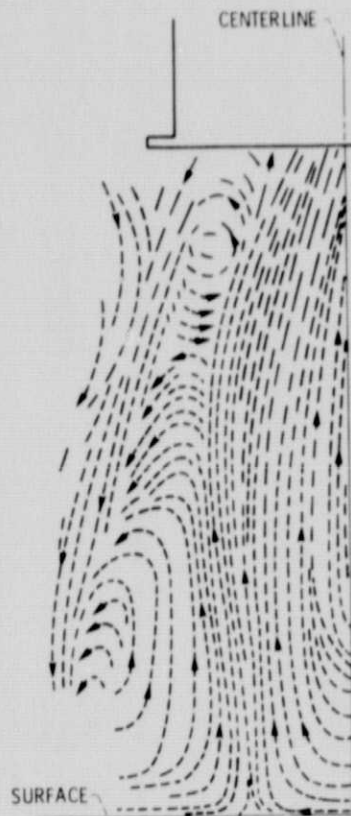
Figure 14. - Experimental flow patterns obtained by Hsu and Fattahi (1975) for a rotating honeycomb above a surface.